

Hydrodynamic Correlations slow down Crystallization of Soft Colloids

D. Roehm,^{1,*} S. Kesselheim,^{1,†} and A. Arnold^{1,‡}

¹*University of Stuttgart, Allmandring 3, 70569 Stuttgart, Germany*

(Dated: June 9, 2021)

Crystallization is often assumed to be a quasi-static process that is unaffected by details of particle transport other than the bulk diffusion coefficient. Therefore colloidal suspensions are frequently argued to be an ideal toy model for experimentally more difficult systems such as metal melts. In this letter, we want to challenge this assumption. To this aim, we have considered molecular dynamics simulations of the crystallization in a suspension of Yukawa-type colloids. In order to investigate the role of hydrodynamic interactions (HIs) mediated by the solvent, we modeled the solvent both implicitly and explicitly, using Langevin dynamics and the fluctuating Lattice Boltzmann method, respectively. Our simulations show a dramatic reduction of the crystal growth velocity due to HIs even at moderate hydrodynamic coupling. A detailed analysis shows that this slowdown is due to the wall-like properties of the crystal surface, which reduces the colloidal diffusion towards the crystal surface by hydrodynamic screening. Crystallization in suspensions therefore differs strongly from pure melts, making them less useful as a toy model than previously thought.

PACS numbers: 64.70.D-, 47.57.E-, 64.75.Xc, 07.05.Tp

Crystallization and nucleation of undercooled melts are often studied using model systems of charged colloids in solution [10, 17, 18], such as polystyrene (PS) or polymethylmethacrylat (PMMA) spheres suspended in water [7, 15, 26]. The solvent gives rise to hydrodynamic interactions (HIs) between the colloidal particles that are not present in, e.g., metal melts. The influence of HIs on the dynamical properties of colloidal suspensions has been extensively studied in recent years [23, 24]. Löwen *et al.* [17, 19] showed that the ratio of the long-time to short-time self-diffusion coefficients has a universal value along the fluid freezing line. Recent studies by Pesche [25] and Nägele [20] of quasi-2D dispersions show that HIs have an impact on the self-diffusion function in these soft-sphere suspensions. However, since crystal growth happens on much larger time scales, it is commonly believed to be a quasi-static process that is unaffected by HIs. For example, in classical nucleation theory (CNT) [14], hydrodynamic interactions are assumed to enter only through the effective diffusion constant of the attaching colloids, which can be measured conveniently in the bulk liquid. Also in most computer simulation studies of nucleation, hydrodynamic interactions are neglected to avoid the high computational costs.

In the following, we will show with the help of computer simulations that HIs do have a remarkable influence on the dynamics of the crystallization in a colloidal suspension. Even at moderate coupling, we found the crystal growth velocity to be reduced by a factor of three. Similar findings have been reported by Schilling *et al.* using different simulations techniques [27].

To investigate the influence of hydrodynamic interactions on crystal growth, we studied the crystallization of Yukawa-type particles confined between two planar walls. The influence of hydrodynamic correlations on crystallization was evaluated by performing both sim-

ulations including and excluding HIs, by employing a fluctuating lattice Boltzmann method [6] and Langevin dynamics [12], respectively. We prepare our systems as an undercooled liquid and let the system crystallize. Due to the presence of the confining walls, the nucleation barrier is sufficiently small, so that we do not need special rare event sampling techniques. All simulations were performed using the MD simulation package *ESPResSo* [4, 5, 28].

As interparticle potential we used a screened Coulomb interaction potential

$$U(r) = l_B k_B T \frac{Q_1 Q_2 \exp(-\lambda_D r)}{r}, \quad (1)$$

where l_B is the Bjerrum length, k_B is the Boltzmann constant, Q_1 and Q_2 give the charges on the interacting particles, r is distance between the particles. The range of the potential is determined by the Debye-Hückel screening length λ_D . The static properties of a Yukawa system can be characterized by two dimensionless parameters [10]

$$\kappa = \frac{w}{\lambda_D} \quad \text{and} \quad \Gamma = \frac{Q_1 Q_2}{4\pi\epsilon_0 w k_B T} = \frac{Q_1 Q_2 l_B}{w}, \quad (2)$$

where $w = (3/(4\pi\rho))^{1/3}$ is the Wigner-Seitz radius of the crystal phase and ρ the particle density. Phase diagrams of systems with Yukawa-type interactions have been calculated both by Monte Carlo simulations [21] and MD simulations [10, 11], which consistently found three regimes: a fluid phase and two different solid phases with BCC or FCC structure, respectively. For our simulations, we chose $\kappa = 3.0$ and $\Gamma = 1260$, which is slightly above the fluid-solid transition line in the BCC regime. The walls act on the particles via a Weeks-Chandler-Andersen (WCA) potential. When modeling the solvent by a Langevin thermostat [3], drag and random forces

on the particles lead to the correct thermal distribution, but hydrodynamic interactions are suppressed. The only tunable parameter is the friction γ , which is inversely proportional to the single particle diffusion constant.

In order to introduce hydrodynamic interactions without simulating the solvent explicitly, we used the lattice Boltzmann method [6] on a three-dimensional (3D) lattice with 19 velocity densities (D3Q19). In all reported simulations with HIs, we used a grid spacing of $g = 1.0$. The NVT ensemble was realized by the fluctuating LB algorithm [1, 29]. We treated the colloidal particles as point particles that are coupled to the LB fluid via a friction term with an adjustable friction constant γ [2]. Note that this friction constant is equivalent to the friction in the Langevin dynamics, which is why we use the same label γ . The no-slip boundaries modeling the fluid-wall interaction were realized by the link bounce back rule [33]. The strength of the hydrodynamic interactions can be quantified by the hydrodynamic radius

$$r_H = \frac{k_B T}{6\pi\eta D^0}, \quad (3)$$

where r_H depends on the viscosity η of the fluid as well as of the single particle diffusion coefficient D^0 , which is inversely proportional to the friction constant γ . In contrast to other methods for including HIs, such as DPD [8, 13], LB methods allow the friction γ to be tuned independently from the viscosity η of the fluid. The particle mobility is not simply the inverse of γ , but also depends on the viscosity η and the lattice spacing of the LB grid due to feedback from the moving fluid [2, 31]. Also, the back flow of the solvent introduces finite-size effects in a system with periodic boundary conditions.

The equations of motion of the Yukawa particles were integrated by a Velocity-Verlet integrator [12]. If not otherwise stated, the simulations were performed with 16,384 particles in a box of size $66 \times 16 \times 16$ confined by two planar walls located at $x = 0.5$ and $x = 65.5$. The time step of the Velocity Verlet integrator was set to $dt = 0.01$, the total simulation length 750,000 time steps. The same time step was also used for the LB fluid update, when applied. As basic length we use the mean particle distance in the crystal phase $a = 1.1$. The time step is $d\tau^* = 0.01\tau$, with $\tau = a\sqrt{k_B T/m_p}$, where m_p is the mass of the colloids. The viscosity is $\eta = 0.8$ and the density of the fluid is $\rho_{fl} = 1.0$ as well as the particle density $\rho = 1.0$. The friction γ varies between 0.5 and 12.5.

The effective diffusion constant depends not only on the applied thermostat, but also on the interactions between the particles. In order to set up comparable simulations, we therefore matched the tracer diffusion coefficient in the bulk liquid. This was done by measuring the MSD of tracer particles in pure bulk systems, both with and without HIs. These measurements were done in 3D periodic systems consisting of 16,384 particles in a

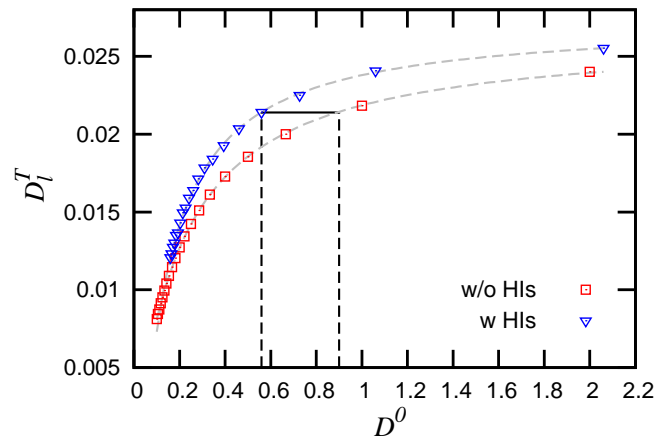


FIG. 1: The diffusion coefficient of the tracer particles in the bulk D_l^T as a function of the single particle diffusion coefficients D^0 . (in simulation units). Red squares show results for the system without HIs and the blue triangles for the systems with HI. The gray dashed lines are a guide to eye. The black lines illustrate the matching of the diffusion coefficient. Two different single particle diffusion D^0 in the Langevin dynamics and the LB coupling result in the same long-time diffusion coefficient D_l^T .

box of size $64 \times 16 \times 16$ without confining walls. Figure 1 shows the measured long-time diffusion coefficient D_l^T of tracer particles in the bulk calculated from the MSD, as a function of the single particle diffusion coefficient D^0 . The simulations with and without HIs led to significantly different tracer diffusion coefficients in the bulk, due to the fact that e.g. the single particle diffusion in case of LB is not simply $D^0 \propto 1/\gamma$ [2]. Furthermore, there is no simple analytical rule to calculate D_l^T in case of a soft-sphere bulk systems. In order to match the tracer particle diffusion coefficient D_l^T , we used different values of γ in the Langevin dynamics and the LB coupling. The black line in Fig. 1 illustrates this matching: in order to obtain the same diffusion coefficient $D_l^T = 0.015$, we have to apply $\gamma = 4.0$ for the Langevin dynamics and $\gamma = 7.0$ for the LB coupling. In the following, we always report data with matched tracer diffusion coefficients in the bulk, where the given values of γ are always the ones that apply to the LB coupling.

Using the matched tracer diffusion, we investigated the freezing of the undercooled fluid confined between two planar walls. In order to distinguish the liquid and the different solid phases, we used the Steinhardt order parameter [30]. Investigations by Moroni *et al.* [22] showed that especially q_4 and q_6 are good choices to determine whether cubic or hexagonal structures are present in the system, respectively. In the following, we will focus on FCC and BCC crystal structures, for which the q_6 order parameter is well suited. Due to

the strong fluctuations in our system, we applied an enhanced averaging method for the Steinhardt order parameter \bar{q}_6 , introduced by Lecher [16]. The literature values are $\bar{q}_6(\text{BCC}) = 0.408018$, $\bar{q}_6(\text{HCP}) = 0.42181$ and $\bar{q}_6(\text{LIQ}) = 0.161962$.

Figure 2 shows the measured \bar{q}_6 of three snapshots taken at different times during a typical simulation run. Note that the points only represent the peaks the distribution of \bar{q}_6 , since in the crystal, there is a strong layering parallel to the wall. In between the peaks, the density drops nearly to zero in the crystal, and consequently so does the order parameter. As expected, the crystal starts with a HCP wall layer, followed by a BCC crystal front that grows with time. To evaluate the position of the crystal front, we fitted the \bar{q}_6 peaks to a function of shape $-h \cdot \arctan((x - s)/w)$, where x is the x -position in the simulation box, h is the height difference between \bar{q}_6 in the liquid and in the FCC phase, w is the width of the liquid-crystal transition region and s is the position of the crystal front. Note that \bar{q}_6 in the liquid bulk is larger than the literature value, since we report only the peaks, not the usual average value.

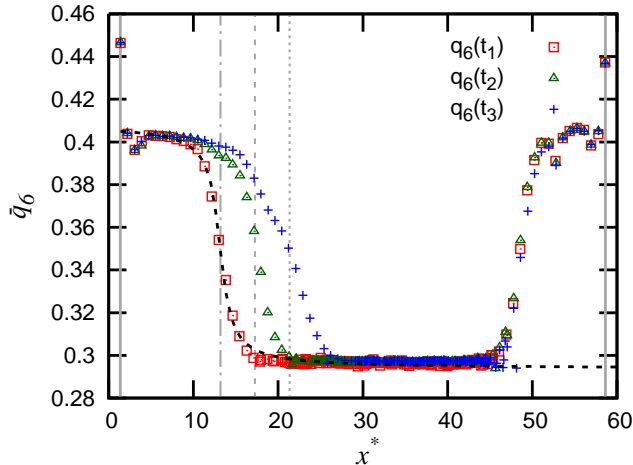


FIG. 2: The figure shows our fitting procedure for s (position of the crystal front), from the function of \bar{q}_6 depending on $x^* = x/a$ for different times $t_1 < t_2 < t_3$. The gray dashed lines indicate the computed front locations ($s_1 < s_2 < s_3$), while the black dashed line shows the fit for s_1 at time t_1 . The symbols represent the peaks of the \bar{q}_6 order parameter.

After some initial time, the crystal grew very uniformly, so that we could determine a constant growth velocity u by a linear fitting of the front position. Figure 3 shows the measured velocities u as a function of the hydrodynamic radius r_H , which we varied by changing the friction coefficient γ and applying the matching procedure described above. Every measurement represents the mean growth velocity sampled from 24 independent runs. For hydrodynamic radii $r_H^* = r_H/a < 0.025$, where

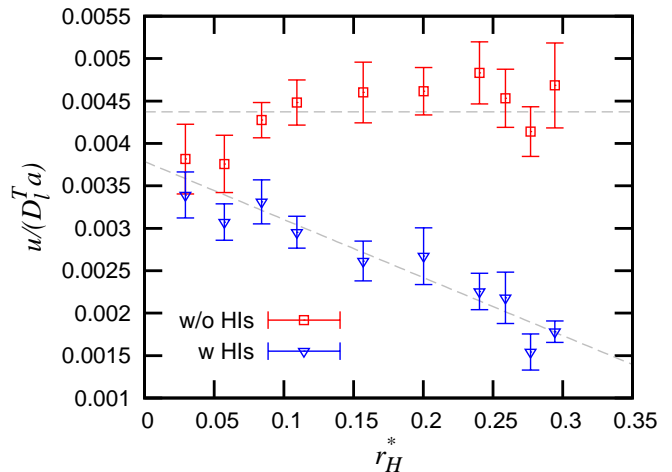


FIG. 3: Growth velocity u normalized by the bulk diffusion coefficient D_l^T times the mean particle distance a as a function of the relative hydrodynamic radius $r_H^* = r_H/a$. The red squares show the results for simulations without HIs, which are almost independent of r_H^* within the error bars. The blue triangles represent the results for simulations with HIs, which show a strong decay of the growth velocity with increasing hydrodynamic radius. The gray dashed lines are guidelines to eye.

a is the mean particle distance in the crystal phase, the influence of HI is almost negligible as one would expect. But already in case of moderate ratios $0.1 < r_H^* < 0.25$, hydrodynamic interactions reduce the crystal growth velocity by up to a factor of 3 at $r_H^* = 0.25$. In case of no HIs the normalized growth velocity is virtually constant, with a decay for small frictions due to improper coupling to the thermostat.

In order to elucidate what causes this difference, we analyzed the particle diffusion in the system relative to the actual position of the crystal front. To accomplish this, we binned our system along the growth direction into bins of width $b = 2a$ and determined the long-time diffusion coefficient D_x^{COM} of the center of mass in the direction of growth, which can be seen as a measure for the transport of particles towards the growing crystal front. In Fig. 4 D_x^{COM} relative to the position of the crystal front x^{rel} , normalized by the center of mass diffusion in the bulk D_v^{COM} of the Langevin simulation is shown. The front of the crystal is located at $x^{rel} = 0$, while the pure bulk fluid phase is located at $x^{rel} = 7$ and the crystal phase is present for $x^{rel} < 0$. As expected, the long-time diffusion coefficients for the center of mass in the crystalline region are almost zero, rise in the region of the crystal front, and settle off to the liquid bulk value far away of the crystal front. The left-hand side of Fig. 4 shows the values for low $r_H^* = r_H/a = 0.025$ ratio, which are virtually the same for both systems: with and

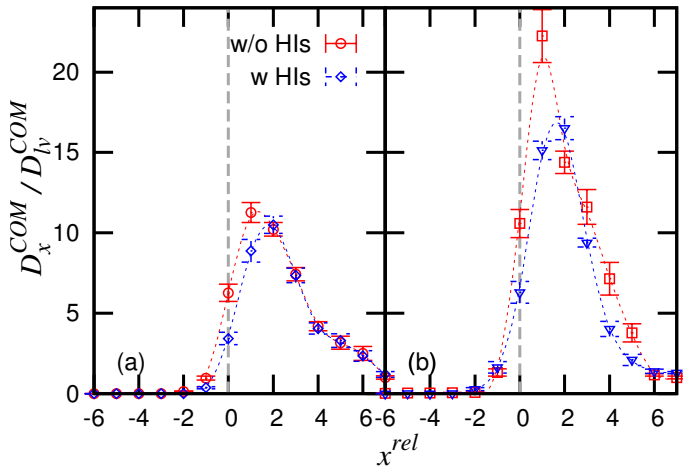


FIG. 4: Long-time diffusion coefficient of the center of mass in the direction of growth. Every value is the long-time diffusion coefficient of the center of mass for particles in a bin of size $b = 2a$ normalized by the value of the Langevin simulation (w/o HIs). The front of the crystal is located at $x^{rel} = 0$, while $x^{rel} = 7$ is located in the pure bulk fluid phase. (a) The first two cases (I: red circles, II: blue rhombus) have a low $r_H^* = r_H/a = 0.025$ ratio and show virtually similar behavior. (b) For moderate $r_H^* = 0.25$, case IV (blue triangles) with HIs shows a different behavior from case III (red squares) without HIs, especially in the region in front of the crystal phase.

without HIs. However, on the right-hand side $r_H^* = 0.25$ is shown, corresponding to moderate hydrodynamic coupling, for which a significantly reduction of the diffusion is present in case of HIs. Especially, nearby the crystal front a drop down of more than a factor of two in the diffusion coefficient occurs, corresponding to a drastically reduced transport towards the crystal. We believe that the reduced diffusion towards the crystal front in the LB system is caused by hydrodynamic screening due to the presence of the wall-like crystal surface. Hydrodynamic screening nearby walls and their influence on the diffusion coefficients parallel and perpendicular to the wall has been reported by Feitosa *et al.* [9] and von Hansen *et al.* [32].

Our simulations show that hydrodynamic interactions have a strong influence on crystallization, even at moderate hydrodynamic radii. Similar finding has been reported by Schilling *et al.* [27] as well. The effects arise mainly on the particle transport towards the crystal front, which are in particular important for nucleation processes. This puts the common assumption into doubt that hydrodynamic interactions can be ignored when studying crystallization or nucleation in suspensions. At least in Yukawa suspensions, these processes do not seem to be quasi-static, and the often drawn analogy to true melts might not be true.

We thank the staff at the Institute for Computational Physics for useful discussions and acknowledge financial

support from the German Science Foundation (DFG) through SFB716 and the cluster of excellence SimTech.

-
- * Electronic address: dominic.roehm@icp.uni-stuttgart.de
† Electronic address: stefan.kesselheim@icp.uni-stuttgart.de
‡ Electronic address: axel.arnold@icp.uni-stuttgart.de
- [1] R. Adhikari, K. Stratford, M.E. Cates, and A.J. Wagner. Fluctuating Lattice Boltzmann. *Euro. Lett.*, 71:473, 2005.
 - [2] P. Ahlrichs and B. Dünweg. Simulation of a single polymer chain in solution by combining lattice Boltzmann and molecular dynamics. *J. Chem. Phys.*, 111(17):8225–8239, 1999.
 - [3] H.C. Andersen. Molecular dynamics simulations at constant pressure and/or temperature. *J. Chem. Phys.*, 72:2384, 1980.
 - [4] A. Arnold, O. Lenz, S. Kesselheim, R. Weeber, F. Fahrenberger, D. Roehm, P. Košovan, and C. Holm. ESPResSo 3.1 — Molecular Dynamics Software for Coarse-Grained Models. In M. Griebel and M. A. Schweitzer, editors, *Meshfree Methods for Partial Differential Equations VI*, volume 89 of *Lecture Notes in Computational Science and Engineering*, pages 1–23. Springer, 2013.
 - [5] A. Arnold, B.A. Mann, H. Limbach, and C. Holm. ESPResSo – An Extensible Simulation Package for Research on Soft Matter Systems. In Kurt Kremer and Volker Macho, editors, *Forschung und wissenschaftliches Rechnen 2003*, volume 63 of *GWDG-Bericht*, pages 43–59. Gesellschaft für wissenschaftliche Datenverarbeitung mbh, Göttingen, Germany, 2004.
 - [6] B. Dünweg and A.J.C. Ladd. Lattice boltzmann simulations of soft matter systems. In *Advanced Computer Simulation Approaches for Soft Matter Sciences III*, volume 221 of *Advances in Polymer Science*, pages 89–166. Springer, Berlin, Germany, 2009.
 - [7] A. Engelbrecht, R. Meneses, and H.J. Schöpe. Heterogeneous and homogeneous crystal nucleation in a colloidal model system of charged spheres at low metastabilities. *Soft Matter*, 7(12):5685–5690, 2011.
 - [8] P. Español and P. Warren. Statistical mechanics of dissipative particle dynamics. *Europhys. Lett.*, 30:191, 1995.
 - [9] M.I.M. Feitosa and O.N. Mesquita. Wall-drag effect on diffusion of colloidal particles near surfaces: a photon correlation study. *Phys. Rev. A*, 44(10):6677, 1991.
 - [10] S. Hamaguchi, R.T. Farouki, and D.H.E. Dubin. Phase diagram of yukawa systems near the one-component-plasma limit revisited. *J. Chem. Phys.*, 105:7641, 1996.
 - [11] S. Hamaguchi, R.T. Farouki, and D.H.E. Dubin. Triple point of yukawa systems. *Phys. Rev. E*, 56(4):4671, 1997.
 - [12] E.J. Hinch. Application of the langevin equation to fluid suspensions. *J. Fluid Mech.*, 72:499–511, 1975.
 - [13] P.J. Hoogerbrugge and J.M.V.A. Koelman. Simulating microscopic hydrodynamic phenomena with dissipative particle dynamics. *Euro. Lett.*, 19(3):155–160, 1992.
 - [14] V. Kalikmanov. Classical nucleation theory. *Nuc. Theory*, pages 17–41, 2013.
 - [15] R. Klein and P. Meakin. Universality in colloid aggregation. *Nature*, 339, 1989.
 - [16] W. Lechner and C. Dellago. Accurate determination of

- crystal structures based on averaged local bond order parameters. *arXiv preprint arXiv:0806.3345*, 2008.
- [17] H. Löwen. Dynamical criterion for two-dimensional freezing. *Phys. Rev. E*, 53(1):29–32, 1996.
 - [18] H. Löwen. Possibilities of phase separation in colloidal suspensions. *Physica A*, 235:129–141, 1997.
 - [19] H. Löwen, T. Palberg, and R. Simon. Dynamical criterion for freezing of colloidal liquids. *Phys. Rev. Lett.*, 70(10):1557–1560, 1993.
 - [20] M.G. McPhie and G. Nägele. Long-time self-diffusion of charged colloidal particles: Electrokinetic and hydrodynamic interaction effects. *J. Chem. Phys.*, 127:034906, 2007.
 - [21] E.J. Meijer and D. Frenkel. Melting line of yukawa system by computer simulation. *J. Chem. Phys.*, 94:2269, 1991.
 - [22] D. Moroni, P.R. Ten Wolde, and P.G. Bolhuis. Interplay between structure and size in a critical crystal nucleus. *Phys. Rev. Lett.*, 94(23):235703, 2005.
 - [23] G. Naegele. On the dynamics and structure of charge-stabilized suspensions. *Phys. Rep.*, 272(5–6):215–372, 1996.
 - [24] J. T. Padding and A. A. Louis. Hydrodynamic interactions and brownian forces in colloidal suspensions: Coarse-graining over time and length scales. *Phys. Rev. E*, 74(3):031402, 2006.
 - [25] R. Pesché, M. Kollmann, and G. Nägele. Brownian dynamics study of dynamic scaling and related freezing criteria in quasi-two-dimensional dispersions. *J. Chem. Phys.*, 114:8701, 2001.
 - [26] D.N. Petsev and N.D. Denkov. Diffusion of charged colloidal particles at low volume fraction: theoretical model and light scattering experiments. *J. Coll. Interf. Sci.*, 149(2):329–344, 1992.
 - [27] M. Radu and T. Schilling. Solvent hydrodynamics affect crystal nucleation in suspensions of colloidal hard-spheres. *arXiv preprint arXiv:1301.5592*, 2013.
 - [28] D. Roehm and A. Arnold. Lattice Boltzmann simulations on GPUs with ESPResSo. *EPJ -ST*, 210:89–100, 2012.
 - [29] U.D. Schiller. *Thermal fluctuations and boundary conditions in the lattice Boltzmann method*. PhD thesis, Johannes Gutenberg-Universität Mainz, 2008.
 - [30] P.J. Steinhardt, D.R. Nelson, and M. Ronchetti. Bond-orientational order in liquids and glasses. *Phys. Rev. B*, 28(2):784, 1983.
 - [31] O.B. Usta, A. J.C. Ladd, and J.E. Butler. Lattice-boltzmann simulations of the dynamics of polymer solutions in periodic and confined geometries. *J. Chem. Phys.*, 122:094902, 2005.
 - [32] Y. von Hansen, M. Hinczewski, and R.R. Netz. Hydrodynamic screening near planar boundaries: Effects on semiflexible polymer dynamics. *J. Chem. Phys.*, 134(23):235102, 2011.
 - [33] D.P. Ziegler. Boundary conditions for lattice boltzmann simulations. *J. Stat. Phys.*, 71:1171–1177, 1993. 10.1007/BF01049965.